Article ID: 1003－6326(2005)05－1031－09

Theoretical analysis of β-$LaNi_5H_x$ ($5 \leqslant x \leqslant 8$): structure and energetics①

LIU Yang(刘 杨), WU Feng(吴 锋)
(National Development Center of Hi-Tech Green Materials, Beijing Institute of Technology, Beijing 100081, China)

Abstract: The calculations of total energy, band structure, and electronic density of states and Mulliken population analysis of β-$LaNi_5H_x$ ($5 \leqslant x \leqslant 8$) were performed by adopting the method of total energy based on the density functional theory. The augmented plane wave function was selected as the basis set in combination with ultra-soft pseudo-potential technology. The influence of the amount of H absorbed in alloys was discussed in terms of geometry, electronic structure and thermodynamic derived from calculated results. The results show that the amount of H absorbed and the preferred site occupation of the absorbed hydrogen atoms were controlled by the position of H-bands and the energy gap between H-bands and conduction bands. The β-phase hydrides of $LaNi_5$ are most stable when hydrogen atom capacity coating in the range of 6－7.

Key words: $LaNi_5$ hydride; geometry; electronic structure; heat of formation
CLC number: TG111; TP139$^+$.7 **Document code:** A

1 INTRODUCTION

$LaNi_5$-based alloys are the negative electrode material widely used in Ni/MH battery presently[1-3]. Many macroscopic prosperities of the material are related with its microscopic structure. It is necessary to properly describe the energy and electronic structure of $LaNi_5$-based alloys and their hydrides. So far, much work on experiment[4-6] and theory[7-12] have been reported. Ultraviolet photoelectron spectroscopy (UPS) was used to measure the electronic specific heat coefficient[4-6] to obtain the electronic change on the Fermi surface before and after alloys hydrogenation. X-ray absorbed near edge spectroscopy (XANES)[7-9] was used to observe the nature of bonds between metal and hydrogen. The calculation method basing on the first principle theory, such as tight binding approximation recursion (TBR)[10], self-consistent linear muffin tin orbital(LMTO)[11] and DV-Xα[12], was adopted to analyse the electron density of $LaNi_5$ and $LaNi_5H_7$. However, the location of the atoms in TBR is in the real space and the periodicity is not considered. And in the atomic sphere approximation of LMTO, the number of the atomic spheres influences the calculated results significantly. Additionally, DV-Xα is based on the cluster and takes only the nearest neighbor atoms into account, so it can hardly pay attention to the influence by farther atoms. In this work, the total energy-plane wave pseudopotential method was introduced with better description of large periodicity system and better analysis to the energy and electronic structure in the hydrogen interstice site in $LaNi_5$.

2 DETAILS OF CALCULATIONS

2.1 Crystal structure

$LaNi_5$ is the parent alloy in AB_5-type hydrogen storage alloys with a hexagonal symmetry (space group P6/mmm, structure type $CaCu_5$). La occupies the 1a (0, 0, 0) site and the two nonequivalent Ni occupy the 2c (1/3, 2/3, 0) and 3g (1/2, 0, 1/2) sites. Two ordered structures about its β-phase hydrides have been reported based on a careful interpretation of the neutron diffraction data. One is P_6/mmm[13] with five nonequivalent interstices available for the hydrogen and their positions are given in Table 1. In the five sites, 3f is octahedron and others are tetrahedron. Another is $P6_3mc$[14, 15], which have a doubled unit cell of $LaNi_5$ along the c-axis and a replacement of the six-fold symmetry axis by a 6_3 screw axis, with three different hydrogen sites (Table 1). In this work, both models were discussed and the initial crystal structures are listed in Table 2 and Table 3.

2.2 Calculation method

The total energy-plane wave pseudo-potential method[16] based on the density functional theory,

① **Foundation item:** Project(2001CCA05000) supported by the National Key Program for Basic Research; Project(2002CB211800) supported by the National Basic Research and Development Program of China **Received date:** 2004－10－20; **Accepted date:** 2005－04－04
Correspondence: WU Feng, Professor, PhD; Tel: +86-10-68912508; Fax: +86-10-68451429; E-mail: wufeng863@vip.sina.com

Table 1 Interstitial sites in unit cell of $LaNi_5$ (space group, $P6/mmm$) and La_2Ni_{10} (space group, $P6_3mc$)

P6/mmm				P6$_3$mc				Coordination
Site	x	y	z	Site	x	y	z	
3f	0.5	0	0	12d	0.47	0	0.058	La×2, Ni^{2c}×2, Ni^{3g}×2
4h	0.333	0.667	0.369	2b	0.333	0.667	0.321	Ni^{2c}×1, Ni^{3g}×3
6m	0.137	2x	0.5	$6c^{I}$	0.138	2x	0.25	La×2, Ni^{3g}×2
12o	0.204	2x	0.354	$6c^{II}$	0.17	2x	0.301	La×1, Ni^{2c}×1, Ni^{3g}×2
12n	0.455	0	0.117					La×1, Ni^{2c}×2, Ni^{3g}×1

Table 2 Position of H in β-$LaNi_5H_x$ unit cell before and after geometry optimization

P6/mmm					P6$_3$mc			
Before	After				Before	After	Before	After
H	$LaNi_5H_5$	$LaNi_5H_6$	$LaNi_5H_7$	$LaNi_5H_8$	H	$La_2Ni_{10}H_{10}$		$La_2Ni_{10}H_{10}$
3f	12o	12n	12n	12n	12d	12d	$6c^{I}$	$6c^{I}$
4h	12o	4h	12o	4h	12d	12d	$6c^{I}$	$6c^{I}$
6m	12o	12o	12o	6m	12d	12d	$6c^{I}$	$6c^{I}$
12o	12n	12n	3f	12o	12d	12d	$6c^{II}$	$6c^{I}$
12n	12n	12o	12o	12n	12d	12d	$6c^{II}$	$6c^{II}$
6m		6m	6m	6m	12d	12d	$6c^{II}$	$6c^{II}$
12o			12o		2b	2b		
12n				12o	2b	2b		
12n				12n				

Table 3 Cell parameters of β-$LaNi_5H_x$

Hydride	a/nm		c/nm		c/a	V/nm^3	
	Model	Calculated	Model	Calculated	Calculated	Model	Calculated
$LaNi_5H_5$	0.539 9	0.542 1	0.429	0.432 7	0.798 2	0.108 3	0.110 4
$LaNi_5H_6$		0.544 1		0.436 9	0.803 0		0.111 3
$LaNi_5H_7$		0.546 3		0.434 9	0.796 1		0.112 3
$LaNi_5H_8$		0.552 8		0.437 8	0.7920		0.115 7
$La_2Ni_{10}H_{14}$	0.539 6	0.545 3	0.857 1	0.865 3	0.793 4	0.216 1	0.222 3

applied for describing the large-scale periodic systems, was adopted. The total energy E_{ks} as a function of electron density $\rho(x)$ can be expressed by

$$E_{ks}[\rho(x)] = T_s[\rho(x)] + E_{es}[\rho(x)] + E_{XC}[\rho(x)] + E_{ext}[\rho(x)] \quad (1)$$

where the terms refer to the kinetic energy T_s of non-interacting electrons, the electrostatic energy E_{es}, the exchange-correlation energy E_{XC}, and the potential energy E_{ext} of non-interacting electrons in the external field.

The generalized gradient approximation (GGA)[17] combined in local density approximation (LDA) was used for the exchange-correlation energy functional. The ultra-soft pseudo-potential (USP)[18] describes the electron-ion interaction and

generates good scattering properties over a pre-specified energy range, which results in much better transferability and accuracy of pseudo-potential. The pseudo-potential basis set in this work comprised a $5s^2 5p^6 5d^1 6s^2$ valence configuration for La, a $3d^8 4s^2$ valence configuration for Ni and a $1s^1$ valence configuration for H. The method for electronic relaxation is based on density mixing[19] combined with conjugate gradient to minimize the sum of eigenvalue. The method is robust for metallic systems for the cell elongated in one dimension. The solution of Kohn-Sham equation can be obtained by self-consistent. The new charge density at the end of the steps mixed with the initial density and the process is repeated until convergence.

In the calculation, the models were transformed to crystalline super-lattice firstly and then geometry optimization was performed on the models in the lowest symmetry (space group, P1). The single energy was calculated on the optimized models. In order to meet the convergence goal, the plane-wave cutoff energy was 240 eV, and the FFT grid was $24 \times 24 \times 18$ for $LaNi_5H_x$ ($x = 5 - 8$) and $24 \times 24 \times 40$ for $La_2Ni_{10}H_{14}$. The calculation was performed in reciprocal space. When the self-consistent process ended, the energy change per atom was less than 0.2×10^{-4} eV/atom, RMS displacement, force and stress was less than 10^{-4} nm, 0.005 eV/nm and 0.1 GPa, respectively. The plane-wave cutoff energy in single point energy calculation was 300 eV, FFT grid was $27 \times 27 \times 24$ for $LaNi_5H_x$ ($x = 5 - 8$) and $27 \times 27 \times 45$ for $La_2Ni_{10}H_{14}$. The k-space is 0.003 5 nm. In the space, according Monkhorst-Pack algorithm, the Γ-centered k-point grids in hexagonal irreducible Brilliouin zones (IBZ) was (6, 6, 7) with 126 k-points for $LaNi_5H_x$ ($x = 5 - 8$) and (6, 6, 3) k-point grids with 98 k-points in IBZ for $La_2Ni_{10}H_{14}$. The simulated environment temperature is 273 K. Calculation of the H_2 molecule was made using a supercell of $0.10 \times 0.10 \times 0.10$ nm^3.

3 RESULTS AND DISCUSSION

3.1 Optimized structures

The cell parameters and the position of hydrogen after optimization are listed in Table 2 and Table 3. Three types of hydrogen motion occur in $LaNi_5H_x$:

1) The tetrahedron sites 4h, 6m and 12o belong to the pentagon ring in a (110) plane[20]. Hydrogen atoms move to 12o site or stay at their original position. It is a fast diffusive motion that can easily occur around the $z = 1/2$ plane, i. e. a hydrogen atom at 6m site move to the 12o site in $LaNi_5H_5$, $LaNi_5H_6$ and $LaNi_5H_7$, and hydrogen at 4h site to the 12o site in $LaNi_5H_5$ and $LaNi_5H_7$. It seems that the only way for a hydrogen atom to escape from a ring of 6m sites is to jump to a 12o site. A hydrogen atom in a 4h site can jump in a z direction to another 4h site, but then it must jump to a 12o site or simply return to its origin, which can be observed in the optimization process.

2) A rapid localized jump happens within the 3f - 12n site clusters consisting of four 12n sites centered on a 3f site of the $z = 0$ plane. It can be understood easily because the distances between nearest-neighbor sites are rather short (3f - 12n, 0.06 nm)[20].

3) The slow diffusive motion can occur between $z = 0$ (3f and 12n sites) and $z = 1/2$ plane (4h, 12o and 6m sites). The diffusion from 12o site to 12n site occur in $LaNi_5H_5$, $LaNi_5H_6$ and $LaNi_5H_7$, and 12n site to 12o site in $LaNi_5H_6$, $LaNi_5H_7$ and $LaNi_5H_8$, and 3f site to 12o site in $LaNi_5H_5$. The only way for a hydrogen atom to escape from the cluster is to jump to a 12o site[21].

In fact, the 12o site seemed to be the "hub" of the process if diffusion occurs by nearest-neighbor jumps, as provided with the experimental study[21]. We can conclude that there must be at least some occupancy of 12o site during absorption. When the amount of hydrogen absorbed varies from 5 to 8, the maximum of hydrogen atoms in 12n site is 3, just as the early experiment results[21].

In $La_2Ni_{10}H_{14}$, the position of hydrogen varies slightly compared with the initial model. The final distribution of hydrogen is 3 at 12d, 2 at $6c^{I}$, 1 at $6c^{II}$, 1 at 2b, which accords with the earlier experiments[22].

It can also be affirmed from Table 3 that with the increase of the amount of hydrogen, the a and c axis increase and the cell volume expanses. The proportions c/a of hydrides lie in the interval 0.792 0 - 0.803 0, quite agreeing with the values $\frac{8-\sqrt{19}}{3\sqrt{3}}$ - $\sqrt{\frac{2}{3}}$[23].

3.2 Electronic structure

3.2.1 Band structures and density of states

Fig. 1 displays the total and partial densities of states (DOS) of $LaNi_5$ and $LaNi_5H_7$ with the Fermi level E_F as the energy zero. As found in earlier theoretical[24-26] and experimental work[27, 28], the occupied bands of $LaNi_5$ and its hydrides are dominantly but not completely filled by Ni-3d bands. They are also hybridized with lanthanum-contributed (6sp-5d) derived states[27] with E_F falling in the rapidly decreasing portion of these bands. There is very little La contribution below E_F and the major La DOS component arises above E_F centered at

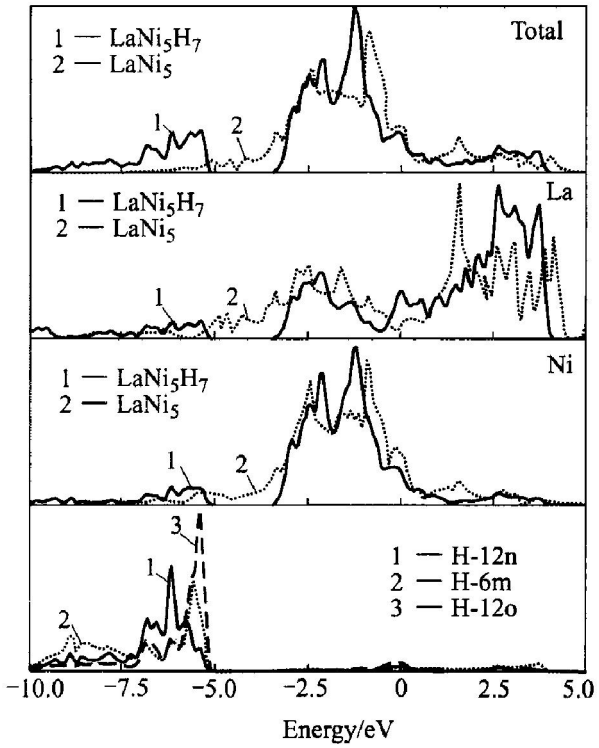

Fig. 1 Total and partial densities of states for $LaNi_5$ and $LaNi_5H_7$(P6/mmm)

1.57 eV in $LaNi_5$ and 2.63 eV in $LaNi_5H_7$, which is from the 4f states according to Ref.[29]. It can be inferred that the small structure observed in the total DOS both in $LaNi_5$ and its hydride arises from the Ni-La interaction. The energy difference between the Ni-3d electrons and the La-5d electrons is so large that the d electrons are more localized on the Ni-sites[30]. With the addition of hydrogen to $LaNi_5$, a new band appeared, lying at a lower energy than the conduction band of the host metal, which can be filled with the added electrons. During the hydrogenation process electrons are progressively transferred from the conduction band of the host metal into this new band, which centers at −5.37 eV. This band involves both the symmetrical (bonding) and the anti-symmetrical (anti-bonding) orbitals derived primarily from the H-1s orbital but with a little d admixture. These states are referred to as hydrogenic states[31]. The hydrogen in $LaNi_5$ hydrides is tending toward the anionic model[32]. The centre of the d-band in hydride shifts downwards from −0.86 eV to −1.25 eV compared with $LaNi_5$, owing to the entry of the protons which lowers the energy of the d band. Additionally, this band narrows from 2.39 eV in $LaNi_5$ to 1.74 eV in $LaNi_5H$ due to the large lattice expansion upon hydrogenation in part and also to the modification of the Ni-3d bands on account of the Ni-H interaction. The narrowing also explains the shape change of the absorption edge in XANES spectra[7]. A very weak structure at low energies due to the M-H bonding is presented in Figs. 1(b) and (c) respectively with a strong Ni-H bonding and a much weaker La-H bond, showing that the hydrogen atoms bind mostly with the nickel atoms[10].

The contour plots (Fig. 2) of the charge densities $\rho(x)$ along the c axis in the $(2\bar{1}\bar{1}0)$ plane of both $LaNi_5$ and $LaNi_5H_7$ (P6/mmm and $P6_3mc$) can also explain it. In Fig. 2(a), the high charge density regions are centered at the Ni atoms in contrast to the low charge density at the interstitial regions, which is well delocalized and not significantly directional, indicative of metallic bonding. A relatively high electron-density region extends from the H site, being located within the corresponding low-density regions of the host alloy, towards the Ni site (Figs. 2(b) and (c)). On the other hand, there is very weak directional La-H bonding in this figure showing the greater importance of the Ni-H interaction than that of the La-H. No localized charge can be detected, suggesting that the local Ni-H interactions would be more ionic than covalent as shown in Ref.[33].

The DOS at Fermi level decreases after hydrogenation (Fig. 3) which is probably caused by filling of the new bonding states formed in these compound with the added electrons of hydrogen and part of excited d electron into empty states in s-p band, indicated in Fig. 4 that the d-orbital distribution to total DOS at E_F reduces with the amount of hydrogen. Whereas the lanthanum d contribution becomes important (Fig. 3 and Fig. 5) as observed in XANES spectra[9], owing to the Fermi level falling in a rising portion of the DOS of the lanthanum valence electrons, while no contribution in $LaNi_5$[34]. What is more, the contribution of La and H to the DOS increases as the amount of hydrogen increases, in contrast to the decrease of Ni.

The position of Fermi level rises with the addition of hydrogen atoms due to the presence of supplementary electron in part brought by added hydrogen atom and also to the deformation of the nickel d bands by the Ni-H interaction (Fig. 6). The δ and d values are plotted in Fig. 7, where δ denotes the distance between the top of H band and the Fermi level E_F, and d denotes the band gap between Hs band and conduction band of hydrides. The trend of δ and d values is similar as hydrogen capacity increases. Furthermore, there exists a knee point when hydrogen equals 7 and when hydrogen is more than 7 the values changes suddenly. It can be speculated that when hydrogen capacity is larger than 7 the hydrides is less stable.

3.2.2 Mulliken population analysis

The ionicity of each atom in $LaNi_5$ and its hydrides was estimated according to the Mulliken

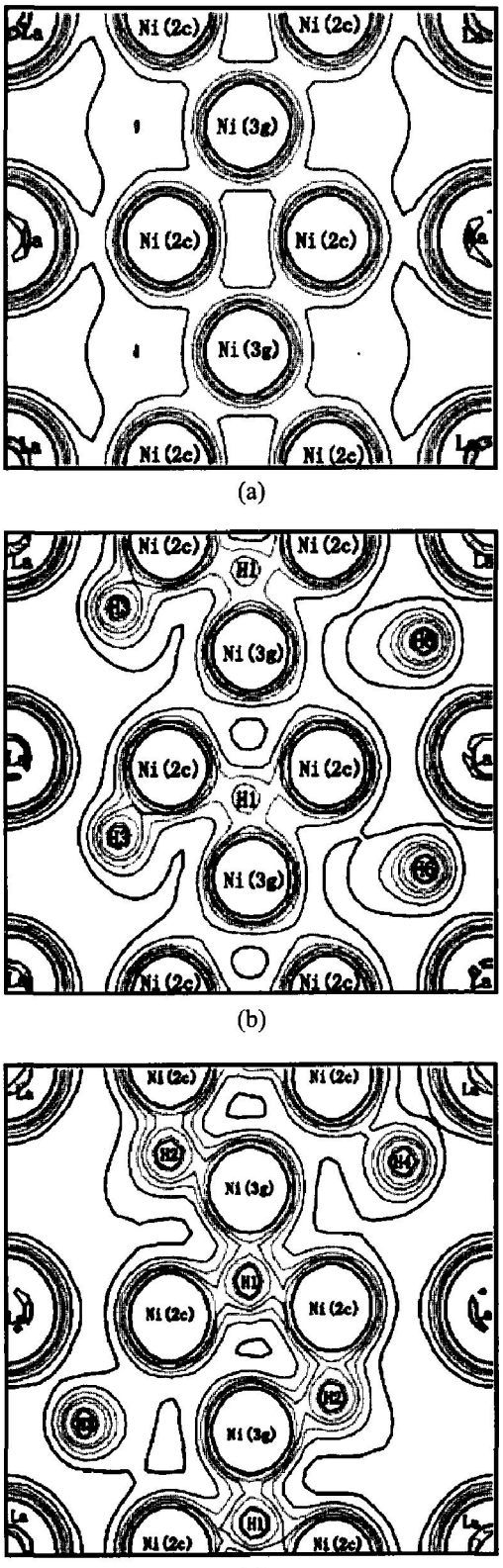

Fig. 2 Valence electron density of $LaNi_5$ (a), $LaNi_5H_7$ ($P6/mmm$) (b) and $La_2Ni_{10}H_{14}$ ($P6_3mc$) (c) for $(2\bar{1}\bar{1}0)$ plane
(Mapping area $2c \times 2c$, inner-most contour 1 079.6 nm^{-3} (0.16a.u.$^{-3}$), outer-most 134.9 nm^{-3} (0.02a.u.$^{-3}$), 134.9 nm^{-3} (0.02a.u.$^{-3}$) step)

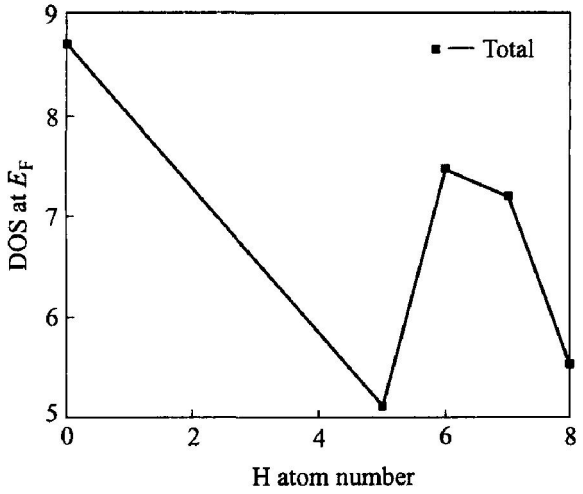

Fig. 3 Variation of DOS at Fermi energy level amount of hydrogen added upon hydrogenation

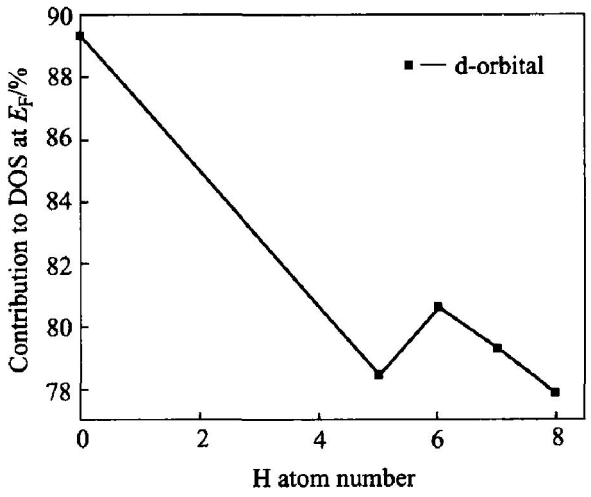

Fig. 4 Contribution of d-orbital to total DOS at Fermi level

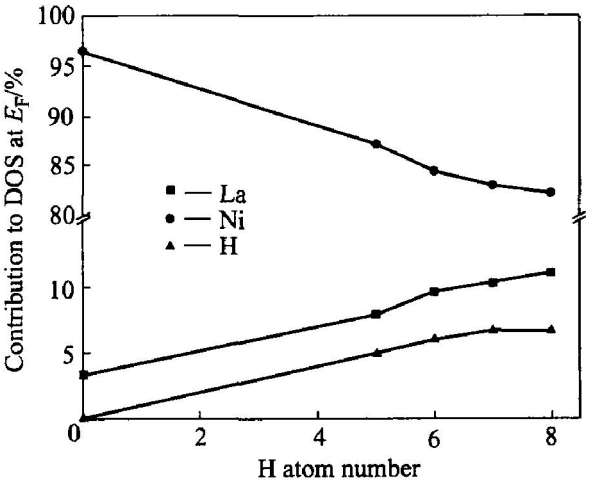

Fig. 5 Contribution of different atoms to total DOS at Fermi level

population analysis. As shown in Fig. 8, the ionicity of the La is always positive. On the other hand, the ionicities of the H and Ni are always negative[33]. The results reveal significant charge transfer from La to Ni and H. As the amount of hydro-

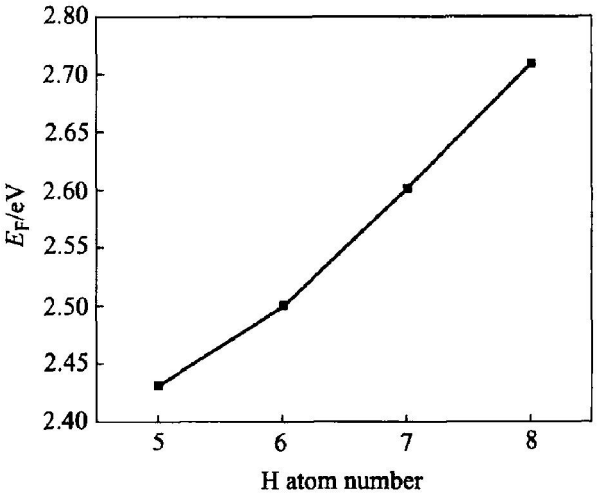

Fig. 6 Position of Fermi energy with different amounts of hydrogen into $LaNi_5$

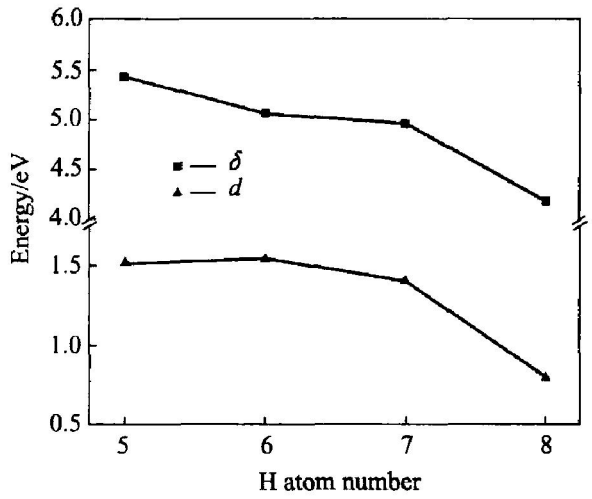

Fig. 7 Changes of δ and d values in $LaNi_5H_x$ (x= 5 - 8)
(δ—Distance between top of H band and Fermi energy E_F; d—Band gap between Hs band and conduction band of hydrides)

gen added increases, the ionicity of H is nearly constant and keeps about 0.3e, whereas, the transferred charge on La increases and the obtained charge on Ni decreases. For example, there is a transfer of about 0.4e per Ni from La to Ni in $LaNi_5$ while only about 0.08e in $LaNi_5H_7$ (P6/mmm and $P6_3mc$). This slightly shifts the d band of hydrides to lower energies because of the decrease in negative charge, which accords with the calculation of DOS shown in Fig. 1.

The bond order is the overlap population of electrons between atoms. This is a measure of the strength of the covalent bond between atoms. The bond order between the hydrogen atom and the La atom is always negative (Fig. 9) regardless of hydrogenation, indicating a repulsive interaction op-

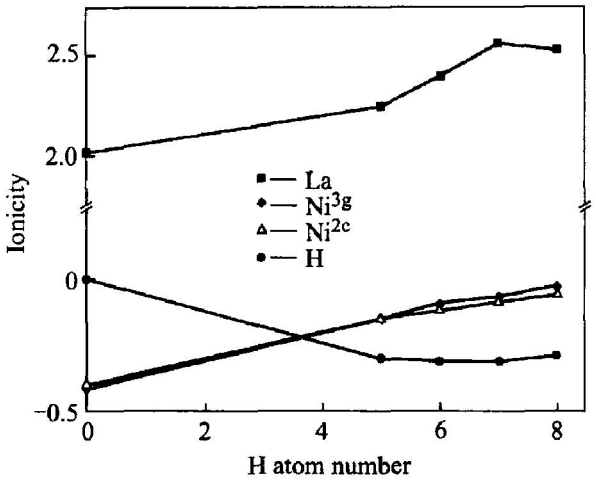

Fig. 8 Changes in ionicities of atoms in $LaNi_5$ and $LaNi_5H_x$ (x= 5 - 8)

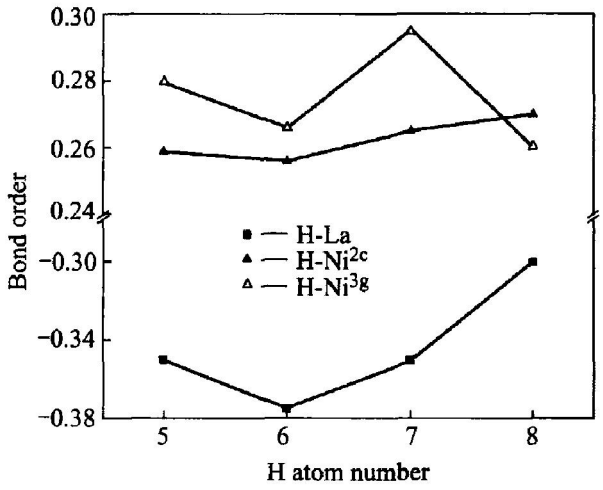

Fig. 9 Changes in bond order of H-metal in $LaNi_5H_x$ (x= 5 - 8)

erating between them. On the other hand, the bond order on Ni-H is always large and positive. It is clear that the hydrogen atom bonds more strongly with the Ni^{3g} atoms than with Ni^{2c} atom except for x= 8 since the ionicity of Ni^{3g} atom is a little higher than Ni^{2c} atom shown in Fig. 8. Likewise, the Ni-H bond is stronger than the La-H bond which is consistent with the result of the electron distribution shown in Fig. 2. It can be also found a knee point at H capacity equal to 7 and after it the bond order changes severely. Fig. 10 shows the change in the bond order between the M-M pairs. The bond order of La-Ni is negative and that of Ni-Ni is positive regardless of hydrogenation. This shows an anti-bonding interaction operating between La and other atoms. Hydrogen atom makes a stronger chemical bond with the Ni atom than with the La atom, despite the larger affinity of La than Ni for hydrogen on the binary metal-hydrogen system. The bond strength between metal pairs is reduced by the introduction of a hydrogen atom into the alloy. Similar results are also reported by

Suenobu et al[7]. A platform can be found between $x = 6$ and $x = 7$. Associated with Fig. 9, it can be inferred that the influence of hydrogen capacity on hydrides is slight with x lying between 6 and 7 and the hydride is stable.

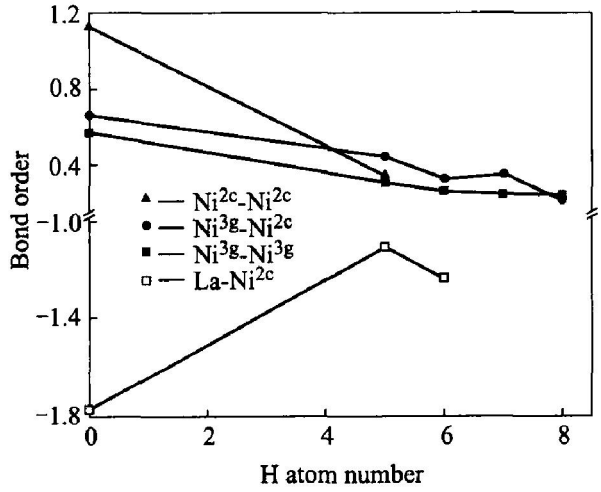

Fig. 10 Changes in bond order of metal-metal in $LaNi_5$ and $LaNi_5H_x$ ($x = 5 - 8$)

3.3 Heat of formation

Heat of formation ΔH is crucial to assessing the practical viability of a hydride material and has been a primary focus of experimental work. Since hydrides are not easily amenable to measurement by experiments, theoretical estimates are of interest and value. Pasturel et al[35, 36] have developed semi-empirical equations to estimate the heat of formation of $LaNi_5$-type hydrides starting from the model of Bouten et al[37] and Mal et al[38]. The ΔH value from this model is − 29.7 kJ/mol. We have calculated the theoretical heat of formation of the hydride directly from the total energies of $LaNi_5$, hydrides and H_2. Table 4 lists the total energies E and heat of formation ΔH obtained from our calculations. Treating all the hydrides with the same computational machinery ensures that systematic errors reduce to the greatest extent in energy differences. The theoretical heat of formation per molecular hydrogen ΔH for the hydrogen reaction, $y LaNi_5 + H_2 = (LaNi_5H_x)_y + \Delta H$ can be calculated as follows[26, 29]:

$$\Delta H = \frac{2}{x}\{\frac{1}{y}[E(MH) - E(M)]\} - E(H_2)$$

It is apparent that $E(H_2)$ is as important to the determination of ΔH as the condensed phase total energies. Including $E(H_{atom})$, the total ground state $E^*(H_2)$ of the H_2 molecule from our computation for a $(1\ nm)^3$ repeated cell is

$$\begin{aligned} E^*(H_2) &= E(H_2) - 2E(H_{atom}) \\ &= -6.795\,0\ eV - 2(12.510\,2\ eV) \\ &= -31.815\,4\ eV \end{aligned}$$

The heat of formation of $LaNi_5H_7$ is the lowest in $LaNi_5H_x$ ($x = 5 - 8$) from Table 4, which shows $LaNi_5H_7$ is the most stable with the amount of hydrogen equal to 7. This result also accords with the suggestion of DOS and Mulliken population analysis. The value (− 35.6 kJ/mol) agrees with calorimetric measurements varying from -32.1 ± 0.1 kJ/mol at 298 K for $LaNi_5H_{6.2}$[39] to -34.8 ± 1.8 kJ/mol at 285 K for $LaNi_5H_{6.33}$[40]. In contrast with the value from the semi-empirical model[38] and from the theoretical calculation by means of the tight-binding linear muffin-tin orbital method[26], this result is closer to the value from experiments. The method in this work is perhaps more creditable and practicable to obtain theoretical heat of formation of $LaNi_5$-type hydrides. When the amount of hydrogen reaches to 7, the heat of formation of the $P6_3mc$ structure is lower than that of P6/mmm, which shows the $P6_3mc$ structure is more reasonable than P6/mmm to β-phase hydrides of $LaNi_5$.

Table 4 Calculated total energies E and heat of formation ΔH

Hydride	E/(eV · f. u.$^{-1}$)	ΔH/(kJ · mol^{-1})
H_2	− 31.815 4	
$LaNi_5$	− 6 152.708 4	
$LaNi_5H_5$	− 6 232.870 1	− 27.9
$LaNi_5H_6$	− 6 249.106 0	− 30.6
$LaNi_5H_7$	− 6 265.353 1	− 35.6
$LaNi_5H_8$	− 6 281.222 7	− 30.2
$La_2Ni_{10}H_{14}$	− 12 530.926 4	− 38.6

4 CONCLUSIONS

By using the super-cell total energy calculation combined with ultra-soft pseudo-potential the geometry and electronic structure and energetics of $LaNi_5$ and $LaNi_5H_x$ ($5 \leqslant x \leqslant 8$) were obtained. The hydrogen motion in β-phase hydrides, including long range diffusion and short range hop, can be observed during the process of geometry optimization as found in experiments. A new band was formed during hydrogenation mainly from the bonding between the hydrogen s orbital and the nickel s-p-d orbital. The band gap between this band and the conduction band can be observed clearly. The calculations reveal the charge transfer from La to Ni and H. The hydrogen takes off the localized La-5d electron near the Fermi level and is mainly inclined to bond with Ni. The calculated total energies can deduce the heat of formation for

$LaNi_5H_x$ ($5 \leqslant x \leqslant 8$), which is very favorable agreement with measurements on $LaNi_5$ hydrides. From the analysis of electronic structure and heat of formation, we can conclude that β-phase hydrides of $LaNi_5$ are most stable when hydrogen atom capacity locating in the range of 6 and 7.

Acknowledge

The authors thank Prof. C. M. Hong of Beijing University and Prof. G. Chen of Jilin University for their helpful discussion for this paper.

REFERENCES

[1] Willems J J G, Buschow K H. From permanent magnets to rechargeable hydride electrodes [J]. J Les-Common Met, 1987, 129(1): 13 - 30.

[2] Bittner H F, Badcook C C. Electrolyte film structure on battery separator and electrode materials [J]. J Electrochem Soc, 1983, 130(2): 259 - 264.

[3] Willems J J G. Metal hydride electrode electrodes stability of $LaNi_5$-related compounds [J]. Philips J Res, 1984, 34(1): 98.

[4] Deenadas C, Thompson A W, Craig R S, et al. Low temperature heat capacities of laves phase lanthanide-aluminum compounds [J]. J Phys Chem Solids, 1971, 32(8): 1853 - 1866.

[5] Takeshita T, Gschneidner K A Jr, Thome D K, et al. Low-temperature heat-capacity study of haucke compounds $CaNi_5$, YNi_5, $LaNi_5$ and $TiNi_5$ [J]. Phy Rev B, 1980, 21(12): 5636 - 5641.

[6] Ohlendorf D, Flotow H E. Experimental heat capacities of $LaNi_5$, α-$LaNi_5H_{0.36}$ and β-$LaNi_5H_{6.39}$ from 5 to 300 K: Thermodynamic properties of the $LaNi_5$-H2 system [J]. J Chem Phys, 1980, 73(6): 2973 - 2948.

[7] Sueenobu T, Sakaguchi H, Adachi G. Studies on local structure in hydrogenated amorphous $LaNi_5$ films using extended X-ray absorption fine structure [J]. J Alloys Comp, 1993, 190(2): 273 - 277.

[8] Suenobu T, Sakaguchi H, Tsuji T, et al. Extended X-ray absorption fine structure studies on local structure in amorphous $LaNi_{5.0}$ films [J]. Bull Chem Soc Jpn, 1991, 64(12): 3522 - 3527.

[9] Tryk D A, Bae I T, Hu Y, et al. In situ X-ray absorption fine structure measurements of $LaNi_5$ electrodes in alkaline electrolytes [J]. J Electrochem Soc, 1995, 142(3): 824 - 828.

[10] Gupta M. Electron properties of $LaNi_5$ and $LaNi_5H_7$ [J]. J Less-Common Met, 1987, 130(1): 219 - 227.

[11] Gupta M. Electronic structure and stability of hydrides of intermetallic compounds [J]. J Alloys and Comp, 1999, 293 - 295(1): 190 - 201.

[12] WEI Wen-lou, GUO Jin, DENG Wen, et al. Correlation between electronic structure of $LaNi_5$ base alloys and hydrogen absorption properties [J]. The Chinese Journal of Nonferrous Metals, 2002, 12(3): 501 - 504.

[13] Percheron-Guégan A, Lartigue C, Achard J C, et al. Neutron and X-ray diffraction profile analyses and structure of $LaNi_5$, $LaNi_{5-x}Al_x$ and $LaNi_{5-x}Mn_x$ intermetallics and their hydrides (Deuterides) [J]. J Less-Common Met, 1980, 74(1): 1 - 12.

[14] Lartigue C, Percheron-Guégan P, Achard J C. Hydrogen (deuterium) ordering in the β-$LaNi_5D_x$ ($x > 5$) phases: a neutron diffraction study [J]. J Less-Common Met, 1985, 113(1): 127 - 148.

[15] Lartigue C, Le Bail A, Percheron-Guégan A. A new study of the structure of $LaNi_5D_{6.7}$ using a modified rietveld method for the refinement of neutron powder diffraction data [J]. J Less-Common Met, 1987, 129(1): 65 - 76.

[16] Payne M C, Teter M P, Allan D C, et al. Interative minimization techniques of ab initio total-energy calculations: molecular dynamics and conjugate gradients [J]. Rev Mod Phys, 1992, 64(4): 1045 - 1097.

[17] Perdew J P, Wang Y. Atoms, molecules, solid and surfaces: applications of the generalized gradient approximation for exchange and correlation [J]. Phys Rev B, 1992, 46(11): 6671 - 6687.

[18] Vanderbilt D. Soft self-consistent pseudopotentials in a generalized eigenvalue formalism [J]. Phys Rev B, 1990, 41(11): 7892 - 7895.

[19] Kresse G, Furthmüller J. Efficient Iterative schemes for Ab-initio total-energy calculations using a plane-wave basis set [J]. Phys Rev B, 1996, 54(16): 11169 - 11186.

[20] Lartigue C, Percheron-Guégan A, Achard J C. Study of the different types of hydrogen motion in the β-$LaNi_{4.5}Al_{0.5}$ hydrides by quasi-elastic neutron scattering [J]. J Less-Common Met, 1984, 101(2): 391 - 403.

[21] Westlake D G. A geometric model for the stoichiometry and interstitial site occupancy in hydrides (deuterides) of $LaNi_5$, $LaNi_4Al$ and $LaNi_4Mn$ [J]. J Less-Common Met, 1983, 91(2): 275 - 292.

[22] Thompson P, Reilly J J, Corliss L M, et al. The crystal structure of $LaNi_5D_7$ [J]. J Phys F Met Phys, 1986, 16(6): 675 - 685.

[23] Gurewitz E, Pinto H, Dariel M P, et al. The structure and dynamics of hydrogen in $LaNi_5H_6$ studied belastic and inelastic neutron scattering [J]. J Phys F: Met Phys, 1983, 13(5): 545 - 554.

[24] Malik S K, Arlinghaus F J, Wallace W E. Calculation of the spin-polarized energy-band structure of $LaNi_5$ and $GdNi_5$ [J]. Phys Rev B, 1982, 25(10): 6488 - 6491.

[25] Sluiter M, Takahashi M, Kawazoe Y. Theoretical study of phase stability in $LaNi_5$-$LaCo_5$ alloys [J]. J Alloys Comp, 1997, 248(1): 90 - 97.

[26] Nakamura H, Nguyen-Manh D, Pettifor D G. Electronic structure and energetics of $LaNi_5$, α-$La_2Ni_{10}H$ and β-$La_2Ni_{10}H_{14}$ [J]. J Alloys Comp, 1998, 281(1): 81 - 91.

[27] Weaver J H, Franciosi A, Wallace W E, et al. Electronic structure and surface oxidation of $LaNi_5$, Er_6Mn_{23}, and related systems [J]. J Appl Phys, 1980, 51(11): 5847 - 5850.

[28] Fuggle J C, Hillebrecht F U, Zelelr R, et al. Electronic structure of Ni and Pd alloys(Ⅰ) —X-ray photoelectron spectroscopy of the valence bands [J]. Phys Rev B, 1982, 27(4): 2145 - 2178.

[29] Hector L G Jr, Herbst J F, Capehart T W. Electronic structure calculations for $LaNi_5$ and $LaNi_5H_7$: energetics and elastic properties [J]. J Alloys Comp, 2003, 353(1): 74 - 85.

[30] Bucur R V, Lupu D. Hydride stability and band structure of the components in the $Pd_{1-x}M_x$ and La-

$Ni_{5-x}Cu_x$ systems [J]. J Less-Common Met, 1983, 90(1): 203 - 209.

[31] Wallace W E, Pourarian F. Photoemission studies of $LaNi_{5-x}Cu_x$ alloys and relation to hydride formation [J]. J Phys Chem, 1982, 86(6): 4958 - 4956.

[32] Wallace W E. Bonding of metal hydrides in relation to the characteristic of hydrogen storage materials [J]. J Less-Common Met, 1982, 88(1): 141 - 157.

[33] Yukawa H, Takahashi Y, Morinaga M. Alloying effects on the electronic structures of $LaNi_5$ containing hydrogen atoms [J]. Intermetallics, 1996, 4 (Suppl 1): S215 - S224.

[34] Chung Y, Takeshita T, McMasters O D, et al. Influence of the lattice and electronic factors on the hydrogenation properties of the RNi_5-base (R is a rare earth) haucke compounds: results of low temperature heat capacity measurements [J]. J Less-Common Met, 1980, 74(1): 217 - 223.

[35] Pasturel A, Chatillon-Colinet C, Percheron-Guégan A, et al. Thermodynamic and structural properties of $LaNi_4M$ compunds and their related hydrides [J]. J Less-Common Met, 1982, 84(1): 73 - 78.

[36] Pasturel A, Liautaud F, Chatillon-Colinet C, et al. Thermodynamic study of the $LaNi_{5-x}Cu_x$ system [J]. J Less-Common Met, 1984, 96(1): 93 - 97.

[37] Bouten P C P, Miedema A R. On the heats of formation of the binary hydrides of transition metals [J]. J Less-Common Met, 1980, 71(1): 147 - 160.

[38] Van Mal H H, Buschow K H J, Miedema A R. Hydrogen absorption in $LaNi_5$ and related compounds: experimental observations and their explanation [J]. J Less-Common Met, 1974, 35(1): 147 - 160.

[39] Hubbard W N, Rawlins P L, Connick P A, et al. The standard enthalpy of formation of $LaNi_5$ and the enthapies of hydriding of $LaNi_{5-x}Al_x$ [J]. J Chem Thermodynam, 1983, 15(4): 785 - 788.

[40] Murray J J, Post M L, Taylor J B. The thermodynamics of the $LaNi_5$-H_2 system by differential heat flow calorimetry (Ⅱ): The α and β single-phase regions [J]. J Less-Common Met, 1981, 80(1): 211 - 219.

(Edited by LI Xiang-qun)